Monte-Carlo-Simulation of Crystallographical Pore Growth in III-V-Semiconductors

Malte LEISNER, Jürgen CARSTENSEN, and Helmut FÖLL

Institute for Materials Science, Christian-Albrechts-University of Kiel, Kaiserstrasse 2, 24143 Kiel, Germany

ml@tf.uni-kiel.de

Abstract – **The growth of crystallographical pores in III-V-semiconductors can be understood in the framework of a simple model, which is based on the assumption that the branching of pores is proportional to the current density at the pore tips. The stochastic nature of this model allows its implementation into a three-dimensional Monte-Carlo-simulation of pore growth. The simulation is able to reproduce the experimentally observed crysto pore structures in III-V-semiconductors in full quantitative detail. The different branching probabilities for different semiconductors, as well as doping levels, can be deduced from the specific passivation behavior of the semiconductor-electrolyte-interface at the pore tips.**

Index Terms – **III-V, crystallographical pores, electrochemical etching, Monte-Carlo-Simulation, InP.**

I. INTRODUCTION

Crystallographical pores (crysto pores) owe their name to their crystallographic growth direction, e.g. the <111>B-direction in III-V-semiconductors, which are the most prominent semiconductor family to feature crysto pores. They have been successfully etched into n-type InP, GaAs, and GaP [1, 2] and show crystallographically defined tetrahedron-shaped pore tips and crystallographical pore walls. Due to the appearance of crystos in several other semiconductors [3, 4], as well as in different electrolytes, the mode of crystallographical pore growth can be seen as a meta feature of pore growth [5]. Therefore crysto pore growth can serve as a model system for the development of a meta model of pore growth. As a starting point, the pore growth in III-V-semiconductors, especially InP, will be considered.

II. EXPERIMENTAL

Samples consisted of (100)-oriented n-type InP and GaAs with different doping levels. All experiments have been carried out in the electrochemical double cell described in [6] at $T = 20$ °C. As electrolyte, 5 wt.% HCl has been used. Experiments have been performed in constant-current-mode with a short 1 s high voltage pulse in the beginning to enable a homogeneous nucleation of pore growth.

III. RESULTS

An example of the resulting crysto pore structures is presented in Fig. 1 for three different etching times in InP with the doping level of $N_D = 8 \cdot 10^{17}$ cm^{-3} and for a constant current density of $j = 0.4$ mA/cm^2. The left hand side shows SEM images of the $(1\bar{1}0)$-plane of the pore structures, the right hand side the corresponding simulation details, as will be discussed in the subsequential part of this manuscript. Crysto pores growing into the two downward pointing <111>B-directions can be identified as lengthy tunnels, whereas pores growing into the two upward pointing <111>B-directions are intersecting the plane of view and are therefore visible as triangular intersection points.

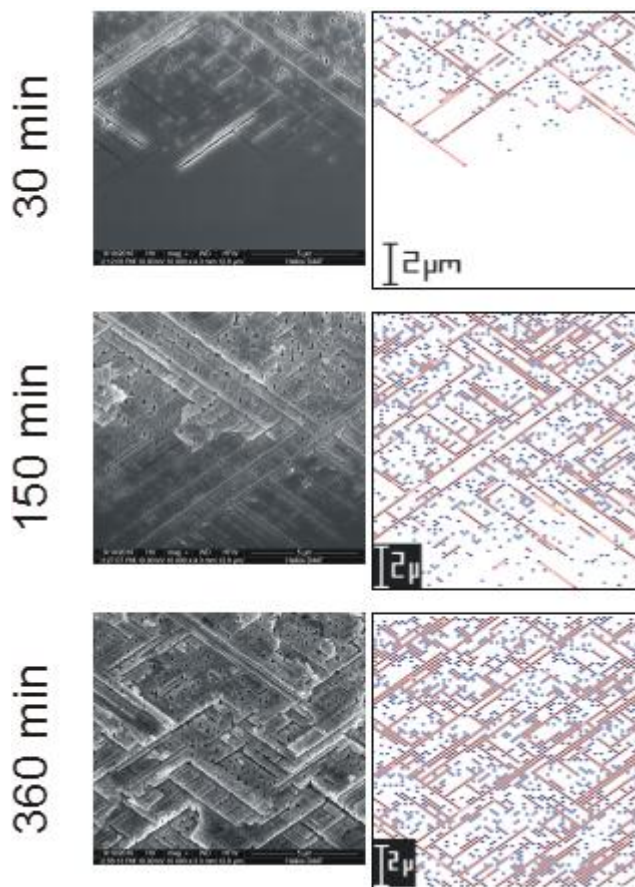
Fig. 1. Resulting crysto pore structures in a constant current experiment, j = 0.4 mA/cm2, on InP with the doping level ND = 8 · 1017 cm-3, $(1\bar{1}0)$-plane. Different etching times are indicated. The left hand side shows SEM images of the pore structure, the right hand side the corresponding simulation result.

Further data has been obtained in these experiments: the pore density of upward and downward growing pores as function of depth, the pore depth as function of time, as well as the number of active pores are all facts which the simulation aims to reproduce. But first a short description of the model which is implemented in the simulation follows.

IV. MODEL

The model basically consists of two assumptions:
i) The branching probability per area and time at the pore

tips p_{tips}, resp. pore walls p_{walls}, is proportional to the current density at the pore tips j_{tips}. Since current density is just charge per time and area, within the current burst model this assumtion can easily be understood as an increased branching probability for short times of interface passivation.

ii) The valence of dissolution is constant, i.e. a constant amount of semiconductor material is etched per unit time.

V. MONTE-CARLO-SIMULATION

The stochastic nature of the above described model allows for its implementation into a three-dimensional Monte-Carlo-Simulation, which has been carried out in a three-dimensional simulation-array, which is schematically illustrated in Fig. 2.
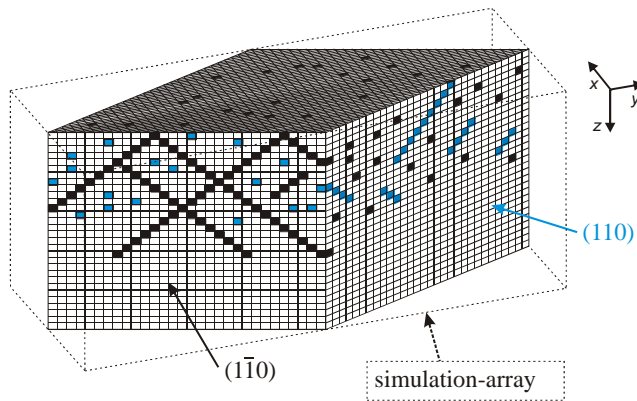

Fig. 2. Schematic illustration of the three-dimensional simulation-array used in the Monte-Carlo-Simulation. The black chains of voxels represent the crysto pores growing into the two upward pointing <111>B-directions respective to the (100)-oriented surface, the blue chains of voxels the crysto pores growing into the two downward pointing <111>B-directions.

The array usually consists of $(1024)^3$ voxels, which can be allocated with different numbers that represent pore walls or tips, which can be active or inactive, and be growing in upward or downward direction. In an initial nucleation routine, pores are randomly distributed in the topmost layers of the nucleation area. The simulation array will then be transformed into a new state in each iteration step according to fixed rules:

1) Each pore grows one more voxel into its growth direction.
2) Branching and growth can only occur into free space, i.e. no other pores are in the trajectory of the growing pore in an adjustable distance called l_{free}.
3) Pores can branch at pore tips, the resulting pore will grow into the same direction (upward resp. downward) as the initial pore. The branching probability per iteration k_{tips} is proportional to the current density at the pore tips j_{tips} and the branching probability per area and time p_{tips}.
4) Pores can branch out of pore walls, the resulting pore will grow into the opposite direction (upward resp. downward) as the initial pore. The branching probability per iteration k_{walls} is proportional to the current density at the pore tips j_{tips} and the branching probability per area and time p_{walls}.
5) If two pore tips meet in one voxel, one tip will continue to grow, whereas the other one will stop to grow.
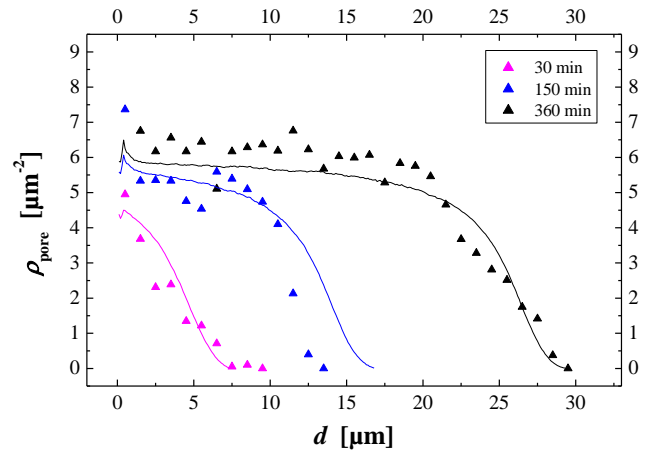
(a)
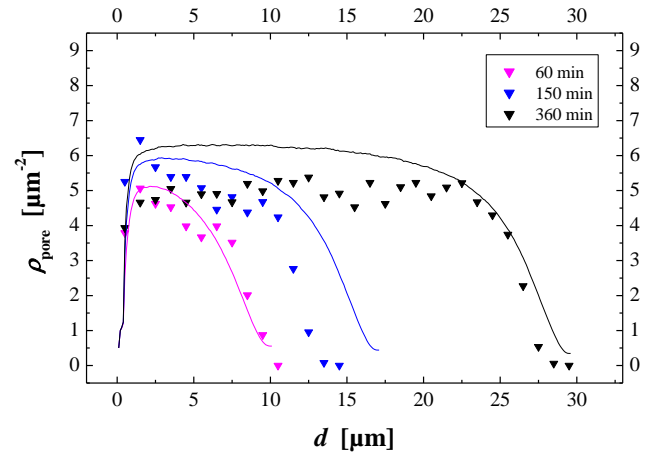
(b)
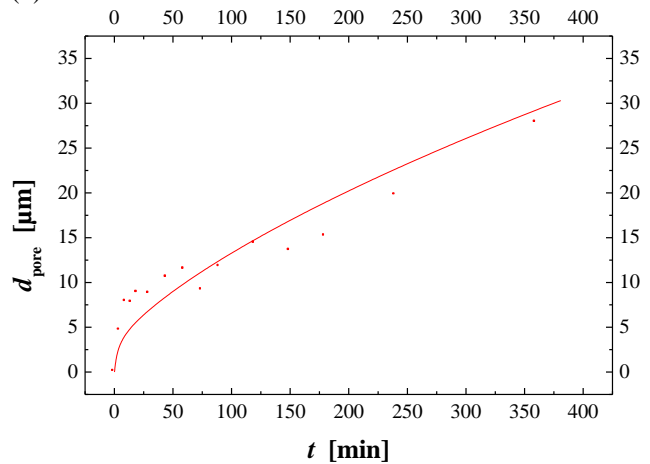
(c)

Fig. 3. Comparison of experiment (dots) and simulation (lines). Pore density ρ_{pore} as function of pore depth of a) upward growing pores and b) downward growing pores for three etching times. c) Pore depth d_{pore} as function of etching time.

6) If branching has occurred at one voxel, no branching can occur out of the neighboring voxels, which will be set to an "inactive" pore wall state. The number of affected neighbor voxels can be adjusted by the parameter l_{pass}.

As already mentioned, Fig. 1 shows the crysto pore structures resulting from the Monte-Carlo-Simulation of crysto pore growth on (100) n-type InP with a doping level of level of $N_D = 8 \cdot 10^{17}$ cm^{-3} and for a constant current density of $j = 0.4$ mA/cm^2. The (1$\bar{1}$0)-plane is shown for

three different etching times besides the respective SEM image of the electrochemically etched pore structure. The similarity between experimental and simulation results is already striking on first view for all shown examples. Similar results have been obtained for the (110)- plane (not shown here). A more quantitative comparison is given in Fig. 3. In Fig. 3a) the pore density ρ_{pore} of upward growing pores is shown as function of depth for three etching times, as evaluated from SEM images (triangles). The lines show the corresponding simulation results. Fig. 3b) shows the respective result for downward growing pores. Fig. 3c) shows a comparison of the pore depth as function of etching time. All simulation results show a very good agreement with the experimental results.

VI. DISCUSSION

In the preceding part of this manuscript it has been demonstrated, that crysto pore growth can be very well modeled by a simple stochastic model which assigns specific probabilities to the branching of pores at pore tips, resp. out of pore walls. For different materials and different doping levels, the branching probabilities per area (W_{tips}, resp. W_{walls}) given in Table 1 have been obtained.

Parameter	InP $8 \cdot 10^{17}$ cm^{-3}	InP $1 \cdot 10^{17}$ cm^{-3}	GaAs $2.5 \cdot 10^{17}$ cm^{-3}
W_{tips} / mm^{-2}	19	59	30
W_{walls} / mm^{-2}	190	22	30

The physico-chemical nature of the branching probabilities can be understood in a simple meta model, which links the branching probability to the passivation behavior of the semiconductor-electrolyte-interface at the pore tips, resp. pore walls. Passivation in this context means the coverage of the surface by chemical species, which impedes current flow and thus electrochemical dissolution. The rather similar values of the normalized branching probabilities for the pore tips can be understood by the fact, that the passivation at the pore tips is rather similar because it is nearly not present, i.e. the pore tips are not passivated.

On the contrary, the increasing normalized branching probability at the pore walls with increasing doping level can be understood by the fact that pore walls are well passivated, which results in the formation of a space-charge-region (SCR) in the semiconductor. A part of the available etching potential can thus drop in the SCR, leaving a decreased etching potential which drops in the electrolyte and is thus available for the electrochemical reaction. Since the potential drop in the SCR decreases with increasing doping level, the potential left in the electrolyte increases with increasing doping level, leading to increasing branching probabilities with increasing doping level.

REFERENCES

[1] T. Takizawa, S. Arai, and M. Nakahara, "Fabrication of vertical and uniform-size porous InP structure by electrochemical anodization", Japan J. Appl. Phys. **137(2, 5A)**, L643 (1994).

[2] H. Föll, S. Langa, J. Carstensen, S. Lölkes, M. Christophersen, and I.M. Tiginyanu, "Review: Pores in III-V Semiconductors", Adv. Mater. **15(3)**, 183 (2003).

[3] V. Lehmann, Electrochemistry of Silicon, Wiley-VCH, Weinheim (2002).

[4] C. Fang, H. Föll, and J. Carstensen, "Electrochemical pore etching in germanium", J. Electroanal. Chem. **589**, 259 (2006).

[5] M. Leisner, H. Föll, and J. Carstensen, "A meta model for electrochemical pore growth in semiconductors", in Nanostructured semiconductors: from basic research to applications, ed. P. Granitzer, Springer (2011).

[6] S. Langa, I.M. Tiginyanu, J. Carstensen, M. Christophersen, and H. Föll, "Formation of porous layers with different morphologies during anodic etching of n-InP", Electrochem. Solid-State Lett. **3(11)**, 514 (2000).